THERMAL PERFORMANCE OF A DUAL-CHANNEL, HELIUM-COOLED, TUNGSTEN HEAT EXCHANGER

Dennis L. Youchison
Sandia National Laboratories
P.O. Box 5800, MS-1129
Albuquerque, NM 87185, USA
(505) 845-3138

Mark T. North
Thermacore, Inc.
780 Eden Road
Lancaster, PA 17601, USA
(717) 569-6551

ABSTRACT

Helium-cooled, refractory heat exchangers are now under consideration for first wall and divertor applications. These refractory devices take advantage of high temperature operation with large delta-Ts to effectively handle high heat fluxes. The high temperature helium can then be used to power a gas turbine for high efficiency power conversion.

Over the last four years, heat removal with helium was shown to increase dramatically when using a porous metal wick by providing a very large effective surface area for heat transfer in a small volume. Last year, the thermal performance of a bare-copper, dual-channel, helium-cooled, porous metal divertor mock-up was evaluated on the 30 kW Electron Beam Test System equipped with a closed helium flow loop at Sandia National Laboratories. The module survived a maximum absorbed heat flux of 34.6 MW/m^2 and reached a maximum surface temperature of 593 ^{o}C for uniform power loading of 3 kW absorbed on a 2-cm^2 area. An absorbed power of 10 kW on an area as large as 24 cm^2 resulted in an absorbed heat flux of 4.2 MW/m^2 and a maximum surface temperature of 602 ^{o}C.

Recently, a similar dual-channel, helium-cooled heat exchanger made almost entirely of tungsten was designed and fabricated by Thermacore, Inc. and tested at Sandia. A complete flow test of each channel was performed to determine the pressure drop characteristics. Each channel of the module was equipped with delta-P transducers and platinum RTDs for independent calorimetry. One mass flow meter monitored the total flow to the heat exchanger, while a second monitored flow in only one of the channels.

The thermal response of the tungsten heat exchanger was obtained to heat fluxes in excess of 5 MW/m^2 using 20 ^{o}C helium at 4 MPa. Fatigue cycles were also performed to assess the fracture toughness of the tungsten module. A description of the module design and new results on flow instabilities are also presented.

I. INTRODUCTION

Over the past five years, dramatic improvements in the power handling capabilities of helium-cooled heat exchangers have occurred due to advanced applications of extended surface technologies such as microchannels and porous metal media. Last year, a dual-channel copper module survived heat fluxes as high as 34.6 MW/m^2 over a 2 cm^2 area reaching a surface temperature of 593 ^{o}C with no evidence of parallel flow instabilities.[1] Effective convective heat transfer coefficients as high as 20,000 W/m^2·K were achieved for this copper device making helium performance comparable to water[2].

Helium-cooled refractory devices are now under consideration that take advantage of high temperature operation with large delta-Ts to utilize the high efficiency power conversion available from new generation gas turbines. It is envisioned that such a heat exchanger can be used as the heat sink on monolithic first wall and tungsten rod-armored divertor components. Such components can accommodate modest heat fluxes by operation at high temperature in the range of 600 ^{o}C to 1500 ^{o}C.

However, operation at high temperature requires that the heat exchanger be made entirely of refractory materials. Unfortunately, refractory metals are brittle and suffer from recrystallization and thermally-induced stress cracking. In addition, economical fabrication of refractory heat exchangers is a difficult undertaking that still requires much development. The use of porous media to enhance heat transfer while minimizing machining costs appears very promising. This article describes the design and fabrication of tungsten heat exchangers by Thermacore, Inc. and Sandia National Laboratories. In addition, the thermal performance, thermal fatigue behavior and the effect of parallel flow instabilities were characterized using the

Electron Beam Test System[3] (EBTS) to provide one-sided heating in excess of 5 MW/m^2.

The development of helium-cooled refractory heat exchangers addressed two major objectives. First, dual modules were designed to handle first wall heat loads and fabricated exclusively of high temperature materials. Secondly, thermal performance and flow instability data were obtained for the new heat exchangers by subjecting them to one-sided heating.

Flow instabilities in the tungsten porous media used in these experiments can be caused by porosity differences in the media of each channel and density reductions due to non-uniform heating. The most important inherent cause of flow bypass in our experiments was the latter. Previous investigations of flow instabilities in a dual-channel, helium-cooled porous metal heat exchanger made entirely of copper revealed that with proper design, flow instabilities would be insignificant even for non-uniform heating. However, refractory devices can operate with much higher inlet temperatures and delta-Ts and order of magnitude higher than copper devices. This leads to even larger reductions in density inside the hot leg and thus a reduction in mass flow. Flow bypass in a parallel cold leg may be a serious concern. The mass flow increases in the colder leg to maintain the same pressure drop. Unfortunately, such a situation decreases the cooling to the hot areas, while increasing it to the cold areas. During plasma disruptions or other off-normal events, such an instability could lead to a catastrophic failure in a helium-cooled plasma facing component.

A Description of the Modules

The dual-channel experiment consisted of two identical helium modules in parallel flow. Each module consisted of a tungsten cylindrical end cap containing a hemispherical shell of brazed tungsten porous metal. This end cap is brazed onto a tungsten cylindrical tube bottomed by a flat tungsten plate that facilitates the brazed attachment of 316 stainless steel supply tubes. The tungsten cylinder acts as the pressure boundary. This cylindrical tube acts as an entrance plenum for the cool helium. The helium flows along the tube walls and enters a hemispherical shell of porous media along its circumference. The helium then flows radially inward while moving closer to the backside of the heated faceplate. At the apex, the flow is redirected normally away from the faceplate along the axis of the hemisphere where it exits the porous media. A stainless steel bellows connects the exit duct to the exit tube at the bottom of the heat exchanger and segregates the hot and cold gas. These components are identified in Fig. 1 which presents a cut-away view of the tungsten heat exchanger. This design minimizes pressure drop by absorbing most of the heat near the exit duct, thus reducing the distance that the hot gas must travel in the porous media and localizing the gas expansion near the exit.

B Assembly of the Modules

All parts for the tungsten heat exchanger including the porous media were fabricated at Thermacore, Inc. However, the final assembly and brazing using a high temperature 11% P 89%Ni (NicroBraze™-10) filler metal were performed at Sandia. The first tungsten module was brazed using a procedure developed by Thermacore. Braze #1 (960 ^{o}C - 5min) attached the stainless steel bellows to the end-cap and the end-cap to the body. Braze #2 (920 ^{o}C - 5min) attached the cup/plug assembly to the stainless steel bellows and the tungsten body, while simultaneously, the stainless steel supply tubes were brazed to the end-cap. Post-braze inspection revealed that there were obvious voids around the stainless steel supply tubes and the end-cap, as well as a large leak. More BNi-6 filler metal was added to the leaky areas, and a rebraze was performed at the same temperature as Braze #2.

Microcracking developed in the braze filler metal (BFM) fillets around the stainless steel tube/end-cap interface. In an effort to seal the micro-cracks, another braze at 980 ^{o}C - 10min was performed. Post-braze inspection revealed that the cracks were still present, as well as the leaks.

In yet another attempt to fill the micro-cracks, BFM (Palcusil™-10) was added, and an additional braze was performed at 900 ^{o}C-10min. The assembly still leaked post-braze, but the leak was substantially smaller. This step was repeated with still additional filler metal until only a small leak could be detected. At that point, a high temperature, vacuum compatible, epoxy resin was used to completely seal the micro-cracks near the supply tubes.

The second tungsten module was fabricated in four separate brazing steps, all using BAu-4 (Nioro™) braze filler metal, either 0.010" or 0.020" diameter wire, in a dry hydrogen atmosphere. Helium mass spectroscopy leak detection was used after each braze step to insure subassembly integrity.

1. The first step was to braze the stainless steel tube assembly to the tungsten end cap. Filler metal

pre-forms were made using 0.020" diameter wire and fitted over the tube/end cap junctions. This braze was accomplished at 1000 ^{o}C for 5 minutes.

2. The next step was to braze the stainless steel bellows assembly to the end cap. Stainless steel fixturing, nickel wire and an alumina rod were used to prohibit inadvertent bellows movement/sagging. Wire pre-forms were used, identical to those in step 1. This braze was performed at 990 ^{o}C for 3 minutes duration.

3. Filler metal (0.020" diameter) pre-forms were placed on the inside diameter of the tungsten body, and positioned against the end cap, after the body was lowered onto the end cap. It was necessary to bend (deform) the bellows slightly to allow the body to seat properly against the end cap. A leak test was performed after this "adjustment", and no leaks were detected. This assembly was brazed at 985 ^{o}C for 5 minutes.

4. The final braze attached the cup/plug subassembly onto the bellows/end cap assembly as identified in Fig. 1. Braze pre forms (0.020" diameter) were made to join the bellows to the tungsten plug, and then the stainless steel tubing/bellows/body/end cap subassembly was pressed onto the plug/cup subassembly. This assembly was strapped into place with nickel ribbon, that was resistance welded to eliminate movement. Finally, both 0.010" and 0.020" diameter were wound into and around the gap between the cup and body. Additional filler metal wire was wrapped around the end cap/body braze joint, where there is, by design, a gap after assembly. Braze temperature was 980 ^{o}C, and the soak time was 5 minutes.

This final assembly passed the helium leak test with no external detectable leaks within our system limitations (1.0×10^{-9} atm cc/sec He).

II EXPERIMENT

A EBTS and HeFL description

A series of thermal response tests were performed on the helium divertor module using the Electron Beam Test System (EBTS) at Sandia National Laboratories. The EBTS, described in detail elsewhere,[3] is a 30 kW, hot cathode, grid-controlled electron beam system operating at 30 kV. The electron beam can be rastered at a frequency of 10 kHz in both the x and y directions and has a spot size of 1.5 mm in diameter. The EBTS is used to study the thermal response and failure modes of high-heat-flux (HHF) materials and components.

The EBTS is equipped with a closed helium coolant loop (HeFL) which can operate at a maximum pressure of 4.1 MPa and temperatures as high as 300 °C.[3] Helium mass flow rates as high as 22 g/s have been achieved for sample pressure drops near 7 kPa and total pressures of 4 MPa. By adjusting the loop blower speed one can produce a constant differential pressure, but cannot provide an arbitrary mass flow rate. The maximum pressure drop for a sample that can maintain a steady flow in the present loop is 55 kPa at 4 MPa.

B Diagnostics

The total mass flow rate in the helium loop is calculated from the pressure drop across an orifice using the local pressure and temperature. This device is referred to as the orifice flow meter. By using this total mass flow and the temperature difference between module inlet and outlet, it is possible to perform calorimetry for both modules.

The dual-channel module was connected with a common inlet and separate outlets for each channel. Each of the channels had a differential pressure transducer for pressure drop comparison. Both of the outlets had a valved connection to the inlet of a turbine volumetric flow meter in the return line. In addition, one channel had a separate valved connection to the outlet of the turbine flow meter. This valve arrangement, shown in Fig. 2, allowed us to control the flow of each of the channels through the flow meter either independently or simultaneously. Unfortunately, the turbine flow meter only operates when the helium flow exceeded 5 g/s at 4 MPa, which was not the case for these modules. However, by applying an identical heat flux over each channel separately and using the proper valving, the system flow, and pressure drop data, we were able to estimate the flow allocation through each channel.

Calorimetry for the two channels was obtained from the partitioned mass flow rate, the pressure drop and the temperature rise of each channel. The temperature rise was determined with the use of three RTD probes inserted in the helium lines, one at the common inlet of the channels and one in each outlet of each channel. Two other thermocouples were attached to the supply tubes ate the bottom of the heat exchangers. These thermocouples were used to measure the bulk temperature during calibration of the optical pyrometers and a 3-12 μm broad-band infrared camera. Two pyrometers with overlapping ranges (150-550°C and 320-1300°C)

were used to measure the surface temperature during heating of the module.

C Procedures

Unheated flow tests were first conducted on the modules to characterize their pre-test condition using helium at 4.0 MPa absolute pressure. First, module #2 was installed in parallel wih a 10-mm-i.d. bypass tube. This permitted enough flow to make use of the turbine flow meter. Each channel was flowed separately. Flow and pressure drop data were accumulated at selected blower speeds for each configuration. While flowing the bypass tube, the turbine flow meter was calibrated to match the flow measured on the Delta-P orifice meter. Conservation of mass was used to deduce the flow in the channel without the turbine meter when in parallel flow.

Thermal response curves for both tungsten modules were obtained by using a heated area of 4.9 cm^2 (2.5 cm in diameter) centered on the 3.2-cm-dia module faceplate. In each case, a circular raster pattern comprised of 8 interlaced concentric circles of carefully selected radii with avarying number of repetitions was created to provide the most uniform heat flux. Module #2 was tested first using flow rates of only 1 to 2 g/s of helium at 4.0 MPa due to its reduced porosity. The helium inlet temperature typically increased from 28 ^oC to 55 ^oC during the test day due to heating from the helium blower motor. The module reached steady state calorimetry in 120 to 150 s at these flowrates. To investigate a worst case scenario for flow bypass, data were obtained for single channel flow through just the module and also for parallel flow using the unheated open bypass tube.

The thermal response test of the first tungsten module was performed with it mounted in parallel with the second module. Prior flow testing indicated that the first module had 30% more porosity than the second. Flow rates of 4 to 5 g/s of helium at 4.0 MPa were attained throughout the thermal response tests. An identical heated area was used with similar applied heat fluxes. Again to investigate flow instabilities, data were obtained for single flow and parallel flow using the other unheated tungsten module.

Finally, thermal fatigue cycles were performed on module #1 at 3.5 To 3.8 MW/m^2 absorbed heat flux. The purpose of these cycles was to investigate stress cracking in the 3-mm-thick tungsten faceplate and possibly reveal other thermal fatigue failure modes. The cycles consisted of 25 s on times where the surface temperature reached about 95% of the steady state temperature. The cooldown time was 10 s.

III RESULTS

A Flow characteristics

A plot of mass flow vs. pressure drop for each flow configuration under isothermal conditions is shown in Fig. 3. For single channel flow, the results indicate that the second module in channel #1 consistently had a pressure drop more than four times higher than the first module in channel #2, most likely due to reduced porosity or clogging. During HHF testing, this difference in flow characteristic led to a pronounced difference on the delta-T produced in the helium and on the surface temperature. However, the porosity difference had a lesser effect on the overall thermal performance and the maximum attainable heat flux.

In the parallel flow configuration, the pressure drop across both modules was approximately 55 kPa with the flow partitioned appropriately between the two modules. This was the maximum target pressure drop achievable with the HeFL at 4 MPa. For the applied head, module #1 garnered about three times the mass flow as module #2, or about 75% of the total flow.

B Thermal response

The thermal response curve for uniform heating on a 4.9 cm^2 area centered on module #2 is shown in Fig. 4. This figure shows data for both single and parallel flow. The maximum heat flux attained for steady state conditions was 5.5 MW/m^2 producing a maximum surface temperature of 934 ^oC during single channel flow. The mass flow rate ranged from 1.1 g/s at the higher heat flux levels up to 1.4 g/s at lower heat fluxes. The maximum delta-T in the helium was 472 ^oC corresponding to a steady state absorbed power in the module of 2700 W.

During parallel flow with a bypass tube, flow redistribution occurred for the highest heat flux levels that resulted in a 39% reduction in flow to the hot leg. The total loop flow dropped by 31% and the bypass flow increased by 8%. This phenomenon is illustrated in the data presented in Fig. 6. An infrared thermagram of the module shown in Fig. 7 presents the temperature distribution across the faceplate for a parallel flow case which exceeded 1000 ^oC on the surface and was terminated before it could reach steady state calorimetry. As expected, the center zone above the exit duct exhibits the

highest surface temperatures. For a 5.1 MW/m^2 heat flux, the surface temperature rose an additional 108 ^{o}C compared to the single channel flow case and the delta-T in the helium increased by 15 ^{o}C. The overall power absorption in the helium decreased to only 63% of the single channel case. For heat fluxes lower than 3 MW/m^2 only minor differences in thermal performance between the two flow configurations were observed.

The thermal response curves for module #1 appears in Fig. 5 below. A maximum heat flux of 5.9 MW/m^2 was absorbed producing a maximum surface temperature of 840 ^{o}C. The mass flow rates during this test sequence ranged from 3 g/s at the higher heat fluxes up to 3.8 g/s under low heat flux. The maximum delta-T in the helium was 189 ^{o}C corresponding to an absorbed steady state power of 2890 W. Virtually identical performance was obtained from the module regardless of whether it was in single channel flow or in parallel flow with module #2. This can be seen in a comparison of temperature distributions between the single and dual flow cases as presented in Fig. 8.

C Thermal fatigue

Module #1 survived over 500 thermal cycles at 3.5 to 3.8 MW/m^2 with a mass flow rate of 3.4 to 3.6 g/s. Module #2 was not cycled because it developed a slight helium leak at the conclusion of its thermal response testing. No difference in the thermal performance of module #1 was noted between the beginning of the cycling and the end. Evidence of microcracking and enhanced porosity of the tungsten in the heated area were observed during post-test inspection. A macroscopic view of the surface presented in Fig. 9 shows the thermal signature created during the thermal response testing of module #1 at the highest heat fluxes. It also shows the presence of braze material on the faceplate that re-flowed above 1000 ^{o}C.

D Post-test inspection

After testing the second module was sectioned longitudinally down the centerline of the porous plug. Fig. 10 is a photograph of the sections. Porosity measurements were made on the module. The average porosity of module #2 was 30%. Fig. 10 presents an optical micrograph of the heated areas and reveals microcracking of the tungsten surface created by cyclic compressive thermal stresses. Excess braze material was also found on the surface.

IV MODELING AND ANALYSIS

To determine the effective heat transfer coefficient inside the divertor module, the module was modeled using the COSMOS/M finite element program.[4] The module was modeled using 2652 4-node tetrahedral elements. Thermal conductivity of the tungsten was taken as XXX W/m·K. Boundary conditions on the module were taken to be adiabatic on all sides except for the inside hemisphere of the plug and the top surface.

Convection to the helium was assumed to be via a constant effective heat transfer coefficient on each of the inside walls of the channels. The local helium temperature was varied linearly along the semi-circumference from the inlet to the outlet using the measured helium inlet and outlet temperatures.

One e-beam shot was modeled in detail using the absorbed heat flux of XXX W/cm^2 on the entire top surface. The heat transfer coefficient on the inside of the porous metal filled channels was varied until the maximum calculated surface temperature matched the temperatures indicated by the thermocouple data. The results of the calculation are shown below in Fig. 11.

Because the helium flow rate through module #2 is lower than module #1, the temperature rise in module #2 is greater than module #1. This suggests that the heat transfer coefficient in module #2 is greater than in module #1. The heat transfer coefficients that matched the thermocouple data were XX,XXX W/m^2·K and XX,XXX W/m^2·K for modules #1 and #2, respectively.

V CONCLUSIONS

It is possible to successfully fabricate a robust, all-refractory helium-cooled heatsink using existing porous metal technology. This high temperature heatsink removed substantial amounts of power even at low mass flow rates by taking advantage of large delta-Ts in the coolant. The heatsink survived over 500 thermal fatigue cycles at 3.5 MW/m^2 with only minimal microcracking of the faceplate. Tungsten rod armor may be incorporated into the tungsten faceplate in advanced pfc designs without the problems of joining dissimilar materials.

These heat exchangers exceeded design specifications and survived a maximum heat flux of almost 6 MW/m^2 and a maximum surface temperature near 1000 ^{o}C. However, the pressure

drop across each module was relatively high, exceeding 55 kPa. There remain problems with controlling porosity and clogging by contaminants. The porosity difference between the two modules in these experiments was as high as 30%.

No evidence of mass flow instabilities was observed for the two modules in parallel even for very high delta-T in the helium. Nearly the same thermal response was obtained on each module. However, for a worst case scenario of an unrestricted flow bypass, a 39% reduction in mass flow occurred in the module resulting in a 42% reduction in power absorbed by the helium.

This level of thermal performance is more than adequate for first wall applications exposed to a 2 MW/m^2 heat flux. However, better performance could be obtained if the porosity could be doubled. This would almost triple the mass flow and power handling capability. Such an innovation could open a design window into the divertor heat flux regime of 20 to 30 MW/m^2 and make high temperature, helium-cooled refractory heatsinks a viable alternative to liquid metal pfcs.

ACKNOWLEDGMENTS

The authors would like to recognize the contributions of K.P. Troncosa and M.E. Miszkiel for operation of the EBTS and helium loop. The authors are also indebted to C.A. Walker for performing a difficult braze procedure and producing a leaktight assembly and A.C. Kilgo for the sectioning and metallography measurements.

Sandia is a multiprogram laboratory operated by Sandia Corporation, a Lockheed Martin Company, for the Department of Energy under Contract DE-AC04-94AL85000.

REFERENCES

1 D.L. Youchison, "Thermal Performance and Flow Instabilities in a Multi-Channel, Helium-Cooled, Porous Metal Divertor Module," *5th Intl. Symp. on Fusion Nucl. Technol.*, Rome, Italy, September 19-24, 1999. *Fusion Engr. & Design*, ***48*** (in press) (2000).

2 D.L. Youchison, M.G. Izenson, C.B. Baxi and J.H. Rosenfeld, "High-Heat-Flux Testing Of Helium-Cooled Heat Exchangers For Fusion Applications," *Fusion Technol.*, **29**, 559 (1996).

3. D.L. Youchison, J.M. McDonald, and L.S. Wold, High Heat Flux Testing Capabilities At Sandia National Laboratories – New Mexico, 1994 Winter Annual Meeting. of the ASME, Heat Transfer in High Heat Flux Systems, HTD-Vol. 301, ASME Book No. G00956, 1994, pp. 31-37.

4. Structural Research and Analysis Corp., Santa Monica, CA, v2.0, January, 1998.

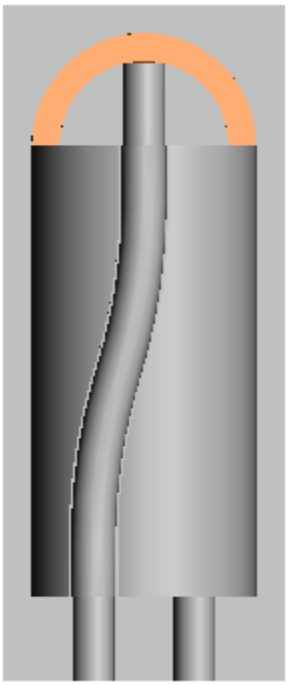

Fig. 1. Two helium-cooled tungsten modules were tested in a parallel flow configuration

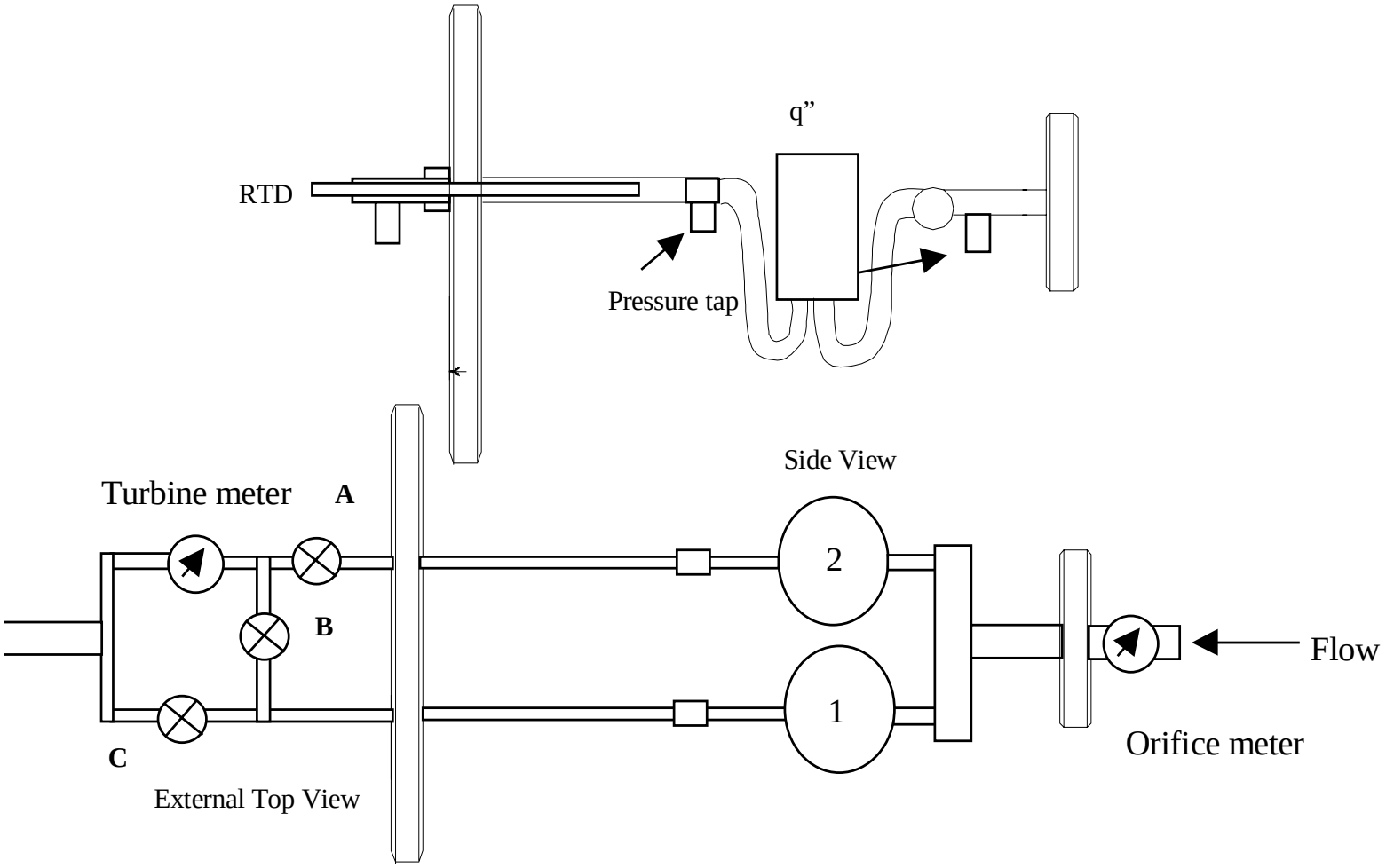

Fig. 2. Three valves were required for flow meter calibration and cross-check. Experiment used close proximity transducers.

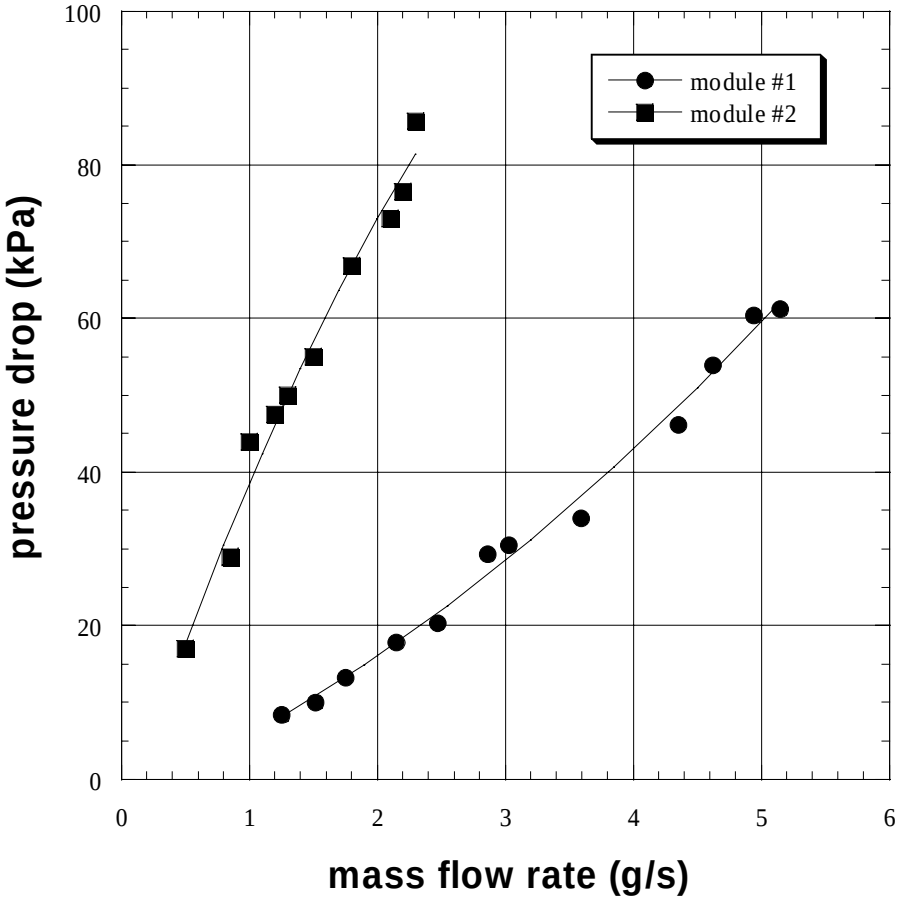

Fig. 3. Flow test results for each module in single channel flow

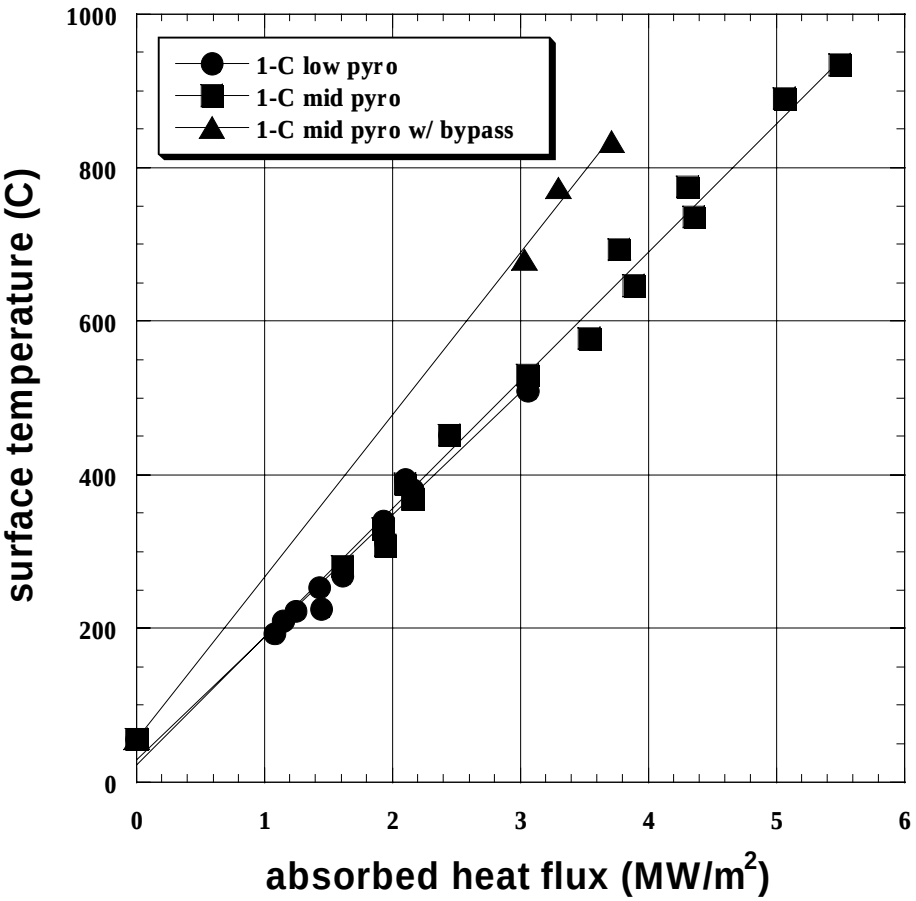

Fig. 4. Surface temperature response for module #2 in single channel flow and with active bypass tube (lines are linear fits to experimental data for single-phase forced convection).

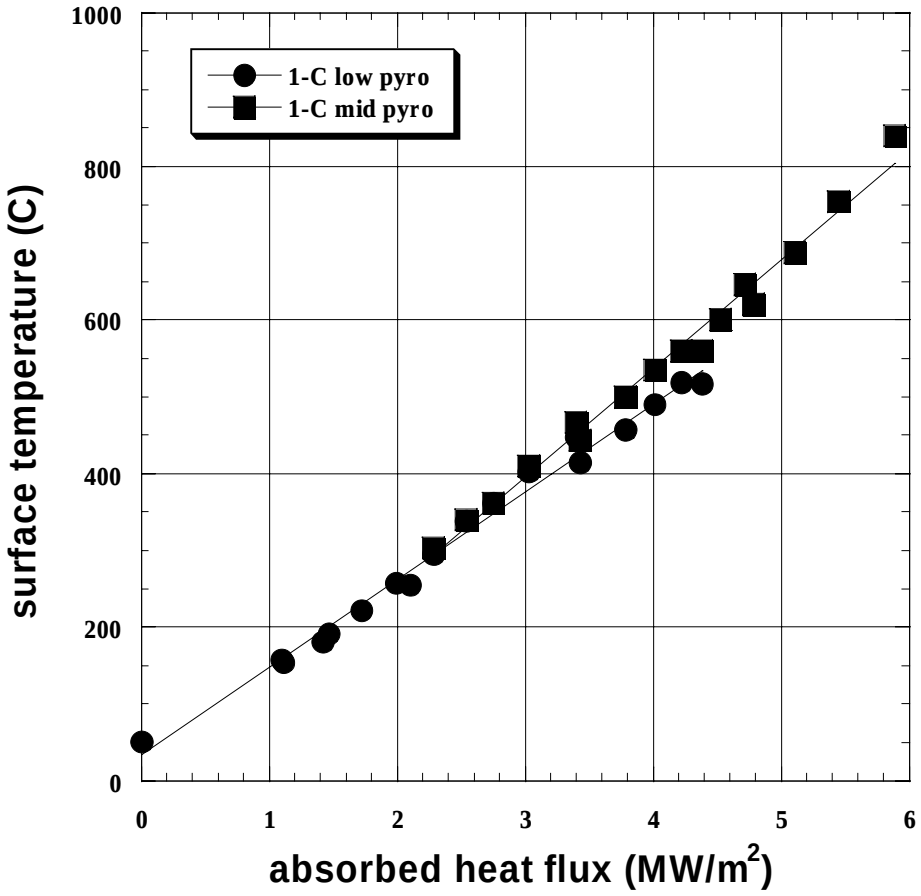

Fig. 5. Surface temperature response for module #1 in parallel flow with unheated module #2 (lines are linear fits to experimental data for single-phase forced convection).

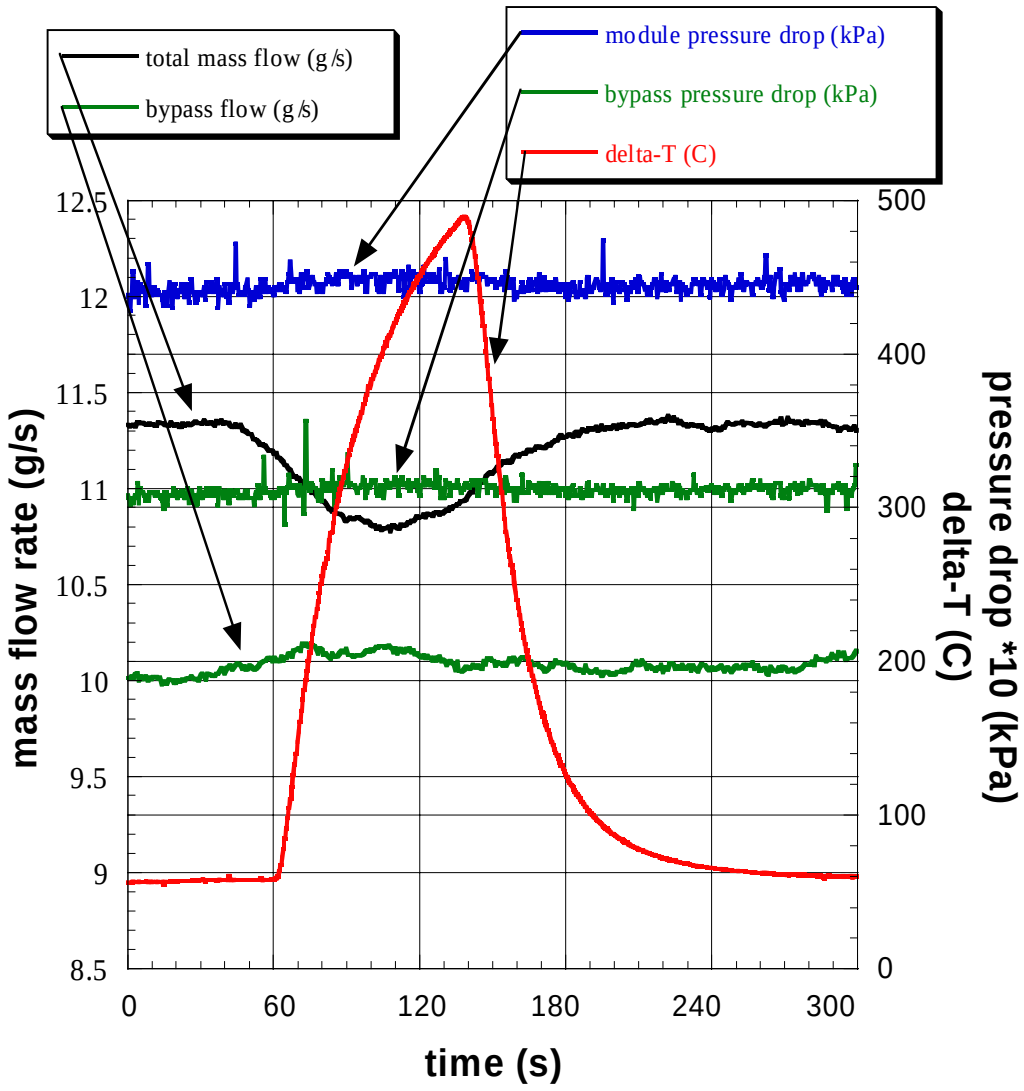

Fig. 6. Evidence of a mass flow instability exists only with a flow bypass tube

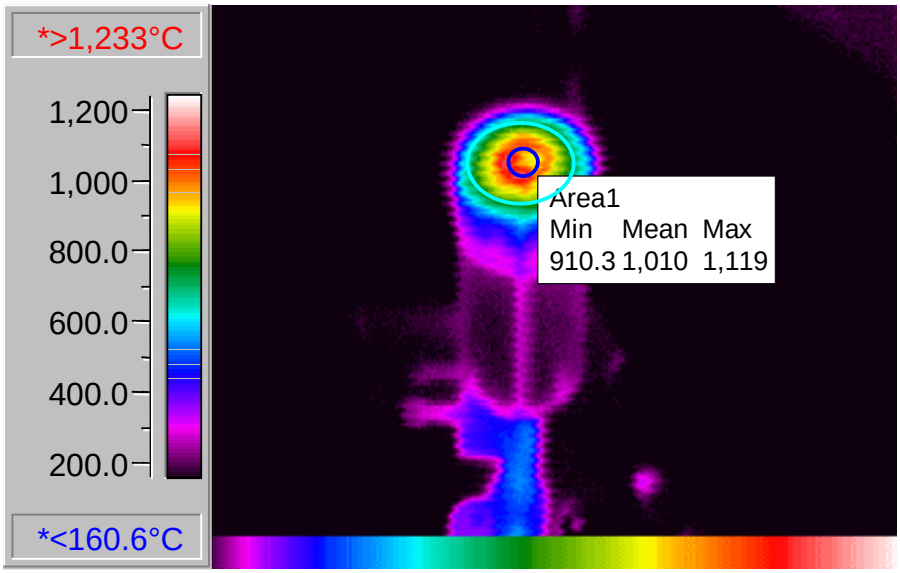

Fig. 7. Temperature distribution on surface of tungsten module at 5.5 MW/m^2.

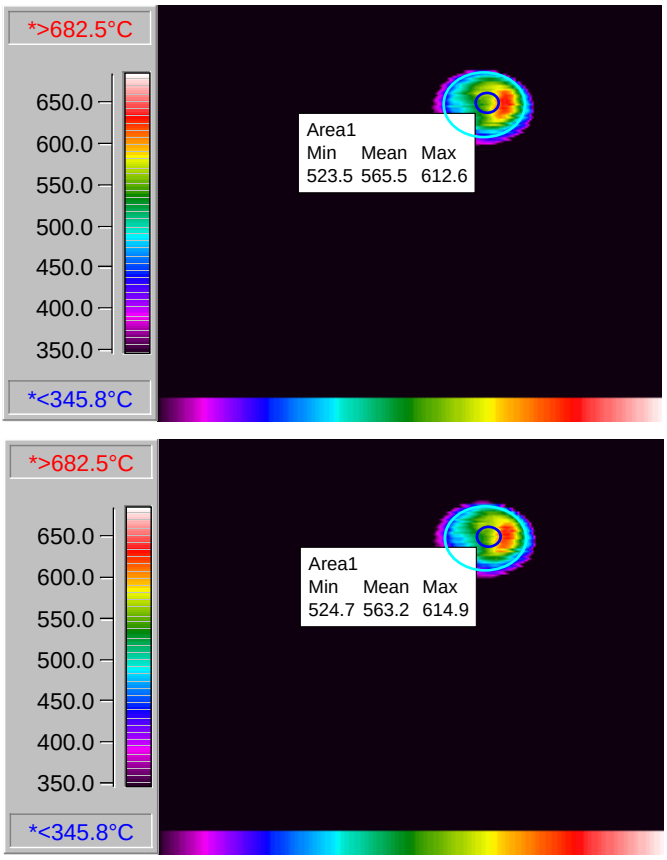

Fig. 8. Temperature distribution on surface of tungsten module #1 for single channel flow (top) and parallel flow (bottom) at 4.3 MW/m^2.

Fig. 9. Post-test photos of modules showing reflow of misplaced braze material on surface.

REPLACE THIS OLD FIGURE

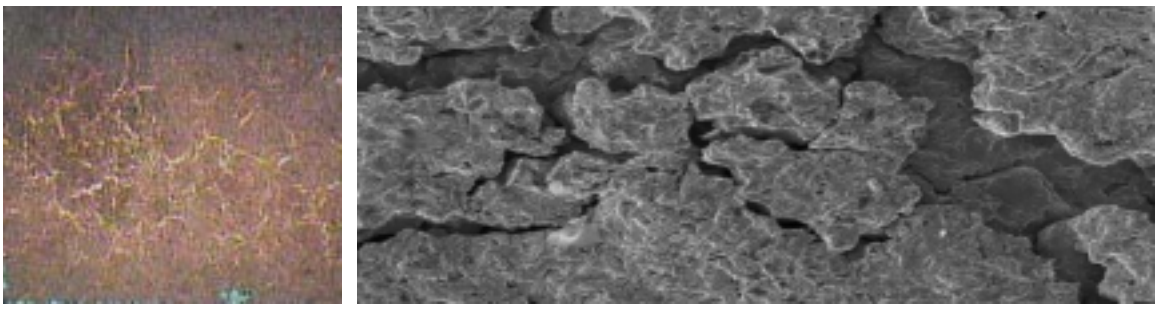

(a) (b)

Fig. 10. Micrographs display surface microcracking of tungsten faceplate due to cyclic thermal stresses: (a) (x10), (b) (x200).

REPLACE THIS OLD FIGURE

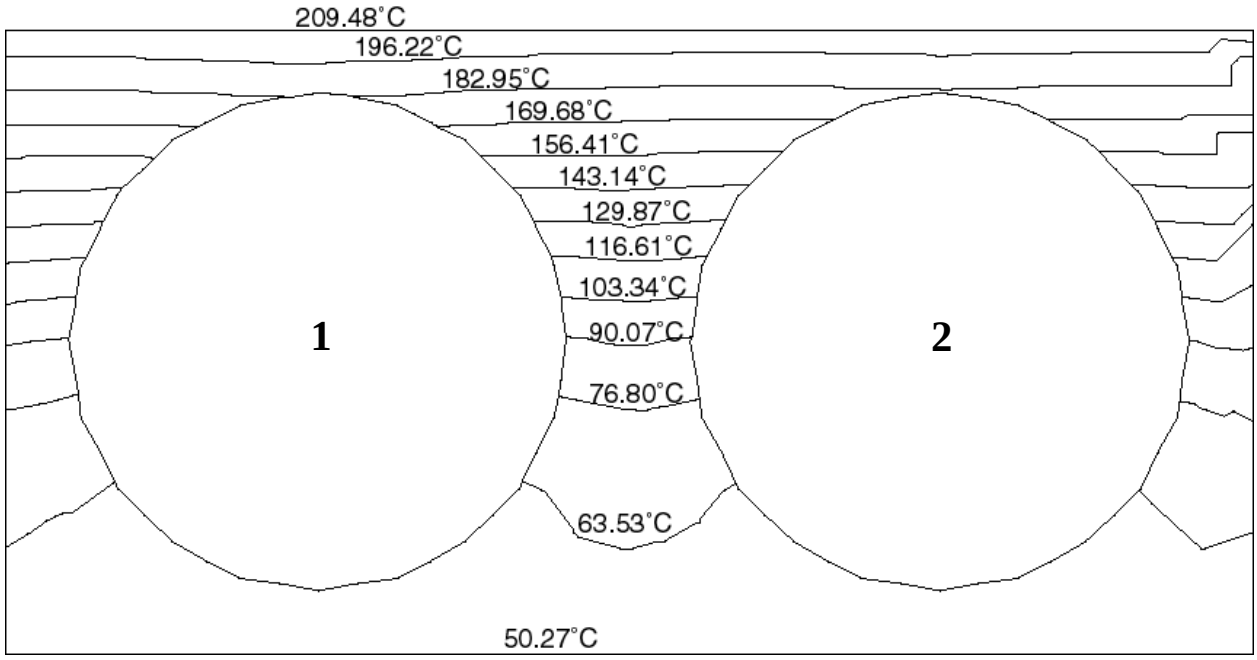

Fig. 11. A steady state temperature profile through the center plane of a module was obtained by numerical modeling. A heat flux of of XXX W/cm^2 applied to the top surface revealed a constant heat transfer coefficient of XX,XXX W/m^2·K on the inside wall of module #1 and XX,XXX W/m^2·K on the inside wall of module #2.